Trichoplein controls microtubule anchoring at the centrosome by binding to Odf2 and ninein

Miho Ibi[1,*], Peng Zou[1,*], Akihito Inoko[1,*], Takashi Shiromizu[1], Makoto Matsuyama[1,2], Yuko Hayashi[1], Masato Enomoto[1,3], Daisuke Mori[4], Shinji Hirotsune[4], Tohru Kiyono[5], Sachiko Tsukita[6], Hidemasa Goto[1,3] and Masaki Inagaki[1,3,‡]

[1]Division of Biochemistry, Aichi Cancer Center Research Institute, Chikusa-ku, Nagoya 464-8681, Japan
[2]The Foundation for Promotion of Cancer Research, Chuo-ku, Tokyo 104-0045, Japan
[3]Department of Cellular Oncology, Graduate School of Medicine, Nagoya University, Showa-ku, Nagoya 466-8550, Japan
[4]Department of Genetic Disease Research, Osaka City University Graduate School of Medicine, Osaka 545-8586, Japan
[5]Virology Division, National Cancer Center Research Institute, Chuo-ku, Tokyo 104-0045, Japan
[6]Laboratory of Biological Science, Graduate School of Frontier Biosciences/Graduate School of Medicine, Osaka University, Suita, Osaka 565-0871, Japan

*These authors contributed equally to this work
‡Author for correspondence (minagaki@aichi-cc.jp)

Accepted 27 October 2010
Journal of Cell Science 124, 857-864

doi:10.1242/jcs.075705

Summary

The keratin cytoskeleton performs several functions in epithelial cells and provides regulated interaction sites for scaffold proteins, including trichoplein. Previously, we found that trichoplein was localized on keratin intermediate filaments and desmosomes in well-differentiated, non-dividing epithelia. Here, we report that trichoplein is widely expressed and has a major function in the correct localization of the centrosomal protein ninein in epithelial and non-epithelial cells. Immunocytochemical analysis also revealed that this protein is concentrated at the subdistal to medial zone of both mother and daughter centrioles. Trichoplein binds the centrosomal proteins Odf2 and ninein, which are localized at the distal to subdistal ends of the mother centriole. Trichoplein depletion abolished the recruitment of ninein, but not Odf2, specifically at the subdistal end. However, Odf2 depletion inhibited the recruitment of trichoplein to a mother centriole, whereas ninein depletion did not. In addition, the depletion of each molecule impaired MT anchoring at the centrosome. These results suggest that trichoplein has a crucial role in MT-anchoring activity at the centrosome in proliferating cells, probably through its complex formation with Odf2 and ninein.

Key words: Trichoplein, Microtubule (MT), Centriole, Odf2, Ninein, Cell proliferation

Introduction

Intermediate filaments (IFs), together with microtubules (MTs) and actin filaments, form the cytoskeletal framework in the cytoplasm of various eukaryotic cells. Unlike MTs and actin filaments, the protein components of IFs vary in a cell-, tissue- and differentiation-dependent manner. Type I and type II keratin proteins form heterodimers in epithelial cells, and their composition also depends on tissue type and the stage of differentiation. Two heterodimers associate with one tetramer, which assembles into higher-order oligomers and forms 10 nm filaments. Keratin IFs associate with plasma membrane specializations such as desmosomes and hemidesmosomes in the periphery. Similarly to other cytoskeletal IFs, keratin IFs also extend into the cytoplasm where they provide a scaffold for other cytoskeletal elements including centrosome and MTs (Eriksson et al., 1992; Steinert, 1993; Fuchs and Weber, 1994; Fuchs and Cleveland, 1998; Magin et al., 2007; Pekny and Lane, 2007; Godsel et al., 2008; Eriksson et al., 2009).

The centrosome is the primary MT-organizing center in animal cells. It is composed of two orthogonal centrioles surrounded by pericentriolar material from which MTs emanate and elongate. These paired centrioles are structurally distinct, reflecting their different ages. The older one (a mother centriole) functions as a template in the preceding cell cycle and carries distal to subdistal appendages, whereas the younger one (a daughter centriole), which is duplicated in the preceding cell cycle, lacks this structure. The mother centriole directly docks MTs at its appendages, whereas the daughter centriole does not (Bornens, 2002; Bettencourt-Dias and Glover, 2007; Bornens, 2008; Nigg and Raff, 2009).

The dynamics of IF network is well correlated with that of other cytoskeletal networks including centrosome and MTs. IF-associated proteins (IFAPs) are emerging as important regulators that coordinate the remodeling and function of such cytoskeletal networks. Members of the plakin family (such as plectin) were identified as crosslinkers between IFs and other cytoskeletal elements including actin filaments and MTs. Although several IFAPs have been identified as regulators of IF remodeling and function, the function of IFAPs in other cytoskeletal systems is largely unknown (Fuchs and Cleveland, 1998; Houseweart and Cleveland, 1998; Izawa and Inagaki, 2006; Godsel et al., 2008).

Nishizawa and colleagues (Nishizawa et al., 2005) previously reported that trichoplein keratin filament-binding protein (trichoplein or TCHP) serves as a keratin IF scaffold protein. Similarly to another keratin IF scaffold protein, Albatross (Sugimoto et al., 2008), this protein has a trichohyalin and plectin homology domain (TPHD; also see supplementary material Fig. S3A), which has similarities to classical keratin IF scaffold proteins (Izawa and Inagaki, 2006). In villous epithelial (non-dividing) cells of the small intestine, trichoplein mainly colocalizes with keratin IFs and the desmosome (Nishizawa et

al., 2005). Here, we report that trichoplein is concentrated at the subdistal to medial zone of both mother and daughter centrioles in dividing epithelial and non-epithelial cells. RNA interference (RNAi)-mediated trichoplein depletion inhibited MT anchoring at the centrosome. This MT-anchoring activity was regulated by the interaction of trichoplein with two other centriole proteins, Odf2 and ninein.

Results and Discussion

We first produced a rabbit polyclonal antibody against full-length (FL) mouse trichoplein. In total cell lysates of EpH4, MTD1A (mouse mammary epithelial) or NIH3T3 (mouse fibroblastic), anti-mouse trichoplein reacted specifically with a band corresponding to mouse trichoplein, which shared 77% homology with human trichoplein (Fig. 1A). Treatment with mouse trichoplein-specific

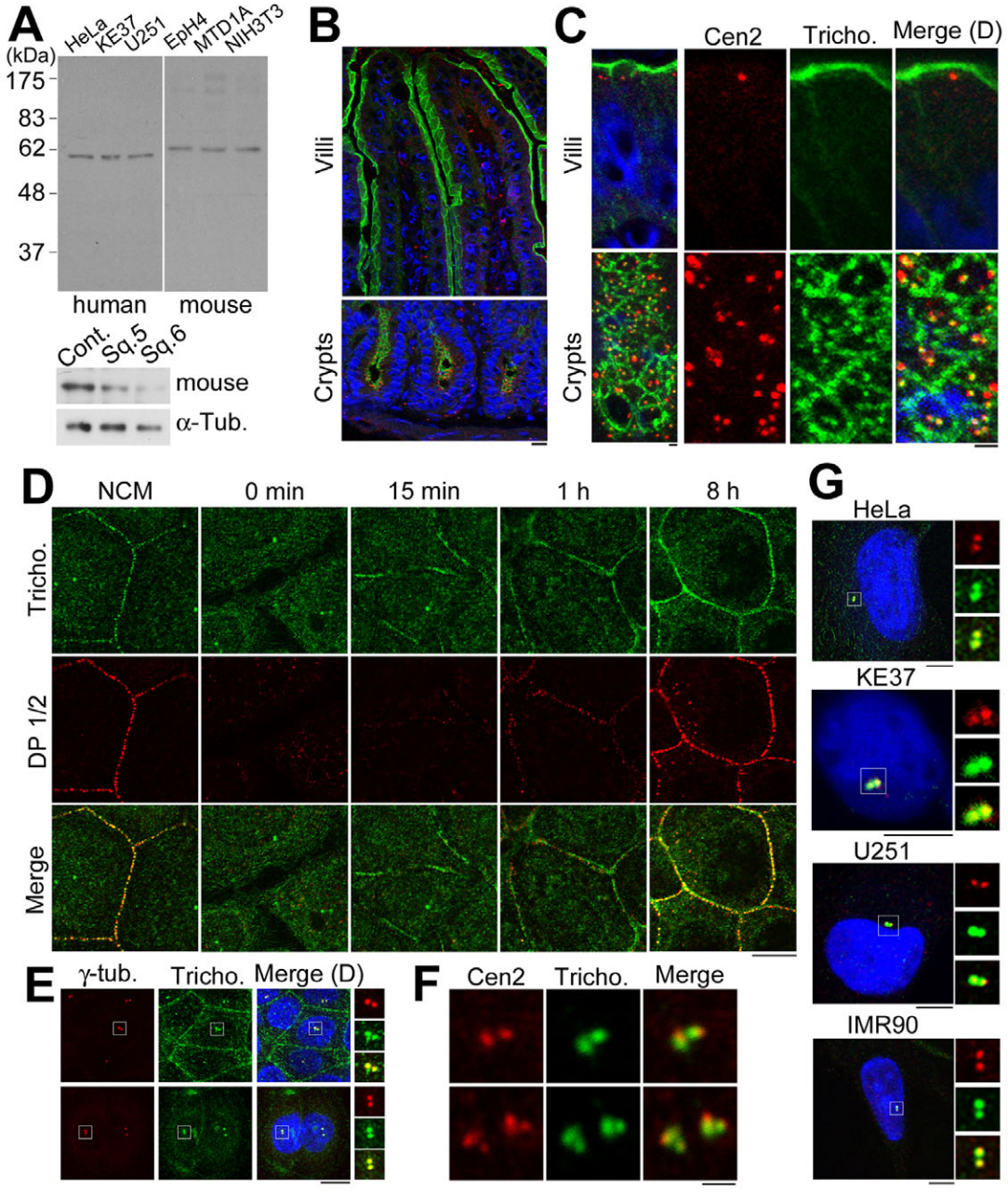

Fig. 1. Trichoplein is localized at the centrosome in proliferating cells. (**A**) Characterization of an anti-human or mouse trichoplein antibody by immunoblotting of indicated cell lysates. In lower panels, EpH4 cells were treated with control (Cont.) or mouse trichoplein-specific siRNA (Sq.5 or Sq.6) for 48 hours. (**B**,**C**) Localization of trichoplein (Tricho.; green) and centrin-2 (Cen2; red) in mouse small intestine. Nuclei were also stained with DAPI (D; blue) in these and subsequent panels. (**D**) Ca^{2+}-switch experiments. MTD1A cells were incubated in low-Ca^{2+} medium (DMEM with 0.05 mM $CaCl_2$) for 17–18 hours and then switched to normal growth medium containing >1.8 mM Ca^{2+} to induce cell junction assembly. Treated cells were subjected to immunocytochemistry with anti-mouse trichoplein and anti-desmoplakin (DP1/2) at the indicated time after switching. NCM indicates cells incubated in normal Ca^{2+} medium containing 10% FBS without the switch. (**E**–**G**) Trichoplein localization in EpH4 (E,F), HeLa, KE37, U251, or IMR90 (G) cells. Red indicates staining with anti-γ-tubulin (E) or anti-centrin-2 (F,G). Boxes in main image indicate centrosome structures shown at high magnification (E,G). Scale bars: 10 μm (B,D,E), 1 μm (C,F), 5 μm (G).

small interfering RNAs (siRNAs) reduced immunoreactivity to this band (Fig. 1A), confirming the specificity of this antibody. We next stained mouse small intestine with the anti-mouse trichoplein antibody. In absorptive epithelial cells, the antibody signals were primarily observed at the cell–cell border where desmoplakin was localized (supplementary material Fig. S1A,B). Especially in the villi, where cells are well differentiated, the signals were also detected as bundles at the apical region (Fig. 1B,C). These staining patterns confirm the previous observation that trichoplein localizes to keratin IFs and desmosomes in the epithelia (Nishizawa et al., 2005).

To elucidate the behavior of trichoplein during the formation of cell–cell attachment, we performed a Ca^{2+}-switch experiment (Fig. 1D). In MTD1A cells, trichoplein was concentrated at the cell–cell contact during cultivation in normal Ca^{2+} medium (NCM); localization of trichoplein almost completely overlapped with desmoplakin in the cell–cell contact area. In low-Ca^{2+} medium, where cell junctions do not form, trichoplein almost disappeared from the cell periphery (Fig. 1D, '0 minutes'). Within 15 minutes of increasing the Ca^{2+} concentration, trichoplein formed a linear structure at the cell–cell contact area. Because it took longer to concentrate desmoplakin in the cell–cell contact area after Ca^{2+} switching (Fig. 1D; also see supplementary material Fig. S1C), trichoplein appeared to have translocated to the cell–cell contact area before desmosome formation. Trichoplein colocalized at the desmosome with desmoplakin at 8 hours after the switch (Fig. 1D).

In addition to keratin IFs and desmosome, trichoplein appeared to localize to anti-centrin-2-positive punctate structures (which implies that they are centrioles) (Paoletti et al., 1996; Laoukili et al., 2000) in the crypt where dividing cells exist (Fig. 1B,C). Such a phenomenon was less observed in the villi where cells cannot divide (Fig. 1B,C). In EpH4 mouse mammary epithelial cells, anti-mouse trichoplein signals overlapped with anti-γ-tubulin-positive spots (which implied centrosomes), although they were also prominent at the cell-cell contact in cells with higher confluency (Fig. 1E). As shown in Fig. 1F, the number of anti-mouse trichoplein signals at the centrosome exactly coincided with the number of anti-centrin 2-positive spots (corresponding to the centriole number). The signals of anti-human trichoplein (Nishizawa et al., 2005) (also characterized in Fig. 1A) overlapped with anti-centrin 2-positive spots in human cultured cells, such as HeLa (cervical carcinoma), KE37 (T-cell leukemia), U251 (glioma) and IMR90 (fibroblast) cells (Fig. 1G). In HeLa cells, which express keratins, the antibody signals were also observed on keratin IFs (supplementary material Fig. S1D), as reported previously

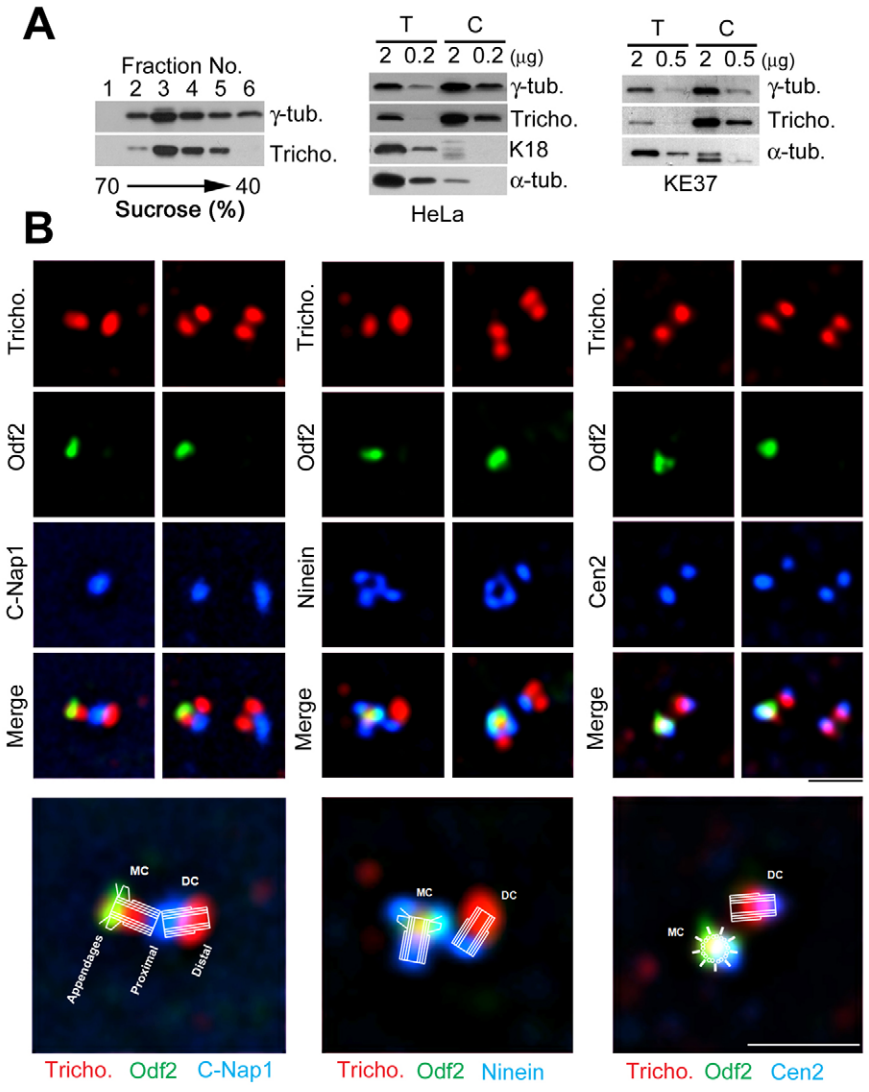

Fig. 2. Trichoplein localizes at the subdistal to medial zone of centrioles. (**A**) Western analyses of centrosomal fractions derived from HeLa (left or middle) or KE37 (right) cells. Each fraction (left), centrosome-enriched fraction (C) or total cell lysate (T; middle or right) was subjected to immunoblotting with the indicated antibodies. The amount of applied protein (μg) is also indicated on the top of each lane (middle or right). (**B**) Comparison of the localization between trichoplein and indicated centriolar marker proteins. Bottom micrographs are shown with cartoons, which indicate the structure of a mother or daughter centriole (MC or DC). Scale bars: 1 μm.

(Nishizawa et al., 2005). To confirm the existence of trichoplein in the centrosome, we prepared centrosomal fractions from HeLa or KE37 cells (Moudjou and Bornens, 1998). As shown in Fig. 2A, trichoplein was enriched in the centrosomal fractions, where γ-tubulin, but not keratin-18 or α-tubulin was concentrated (Fig. 2A). All these observations suggest that trichoplein is ubiquitous in both mother and daughter centrioles at a proliferative phase of the cell cycle.

To examine more precisely the localization of trichoplein on the centriole, HeLa cells were stained with several centriolar markers, together with anti-human trichoplein (Fig. 2B). One of the trichoplein signals partially overlapped signals of an antibody against Odf2 (outer dense fiber protein 2), a protein with distal to subdistal appendages on the mother centriole (Lange and Gull, 1995; Nakagawa et al., 2001; Ishikawa et al., 2005). However, the centriolar localization of trichoplein was different from that of C-Nap1 (centrosome-associated protein CEP250) (Fig. 2B, left panels), which localizes to the proximal ends of centrioles (Fry et al., 1998; Mayor et al., 2000). Anti-ninein signals were detected as four dots (Fig. 2B, middle panels), corroborating previous reports that ninein is localized not only at subdistal appendages of a mother centriole, but also at its proximal end (Mogensen et al., 2000; Ou et al., 2002; Delgehyr et al., 2005). Trichoplein signals were observed among three dots of anti-ninein signals (Fig. 2B, middle panels), which probably represent signals at subdistal appendages and the proximal end of a mother centriole (Fig. 2B, bottom micrographs with a cartoon). In addition, trichoplein partially overlapped with centrin-2 (Fig. 2B, right panels; also see Fig. 1F), a protein found at the distal ends of centrioles (Paoletti et al., 1996; Laoukili et al., 2000). All these results suggest that trichoplein is localizes to the subdistal to medial zone of a mother or daughter centriole.

This specific localization raised the question as to whether trichoplein interacts with ninein and Odf2. We first transfected COS7 cells with His-tagged trichoplein and GFP-tagged ninein and Odf2. His–trichoplein and each GFP-tagged protein were co-immunoprecipitated using an anti-GFP antibody (supplementary material Fig. S2A) and co-purified by Ni-NTA affinity chromatography (supplementary material Fig. S2B). Yeast two-hybrid analyses confirmed an interaction of trichoplein with ninein and Odf2 (supplementary material Fig. S3A), which was similar to that with keratin IF (Nishizawa et al., 2005). Immunoprecipitation analysis using an anti-human trichoplein antibody revealed that endogenous trichoplein formed a complex with endogenous ninein and Odf2 (Fig. 3A). GST pull-down assays using each purified protein indicated that trichoplein directly bound Odf2β (also called

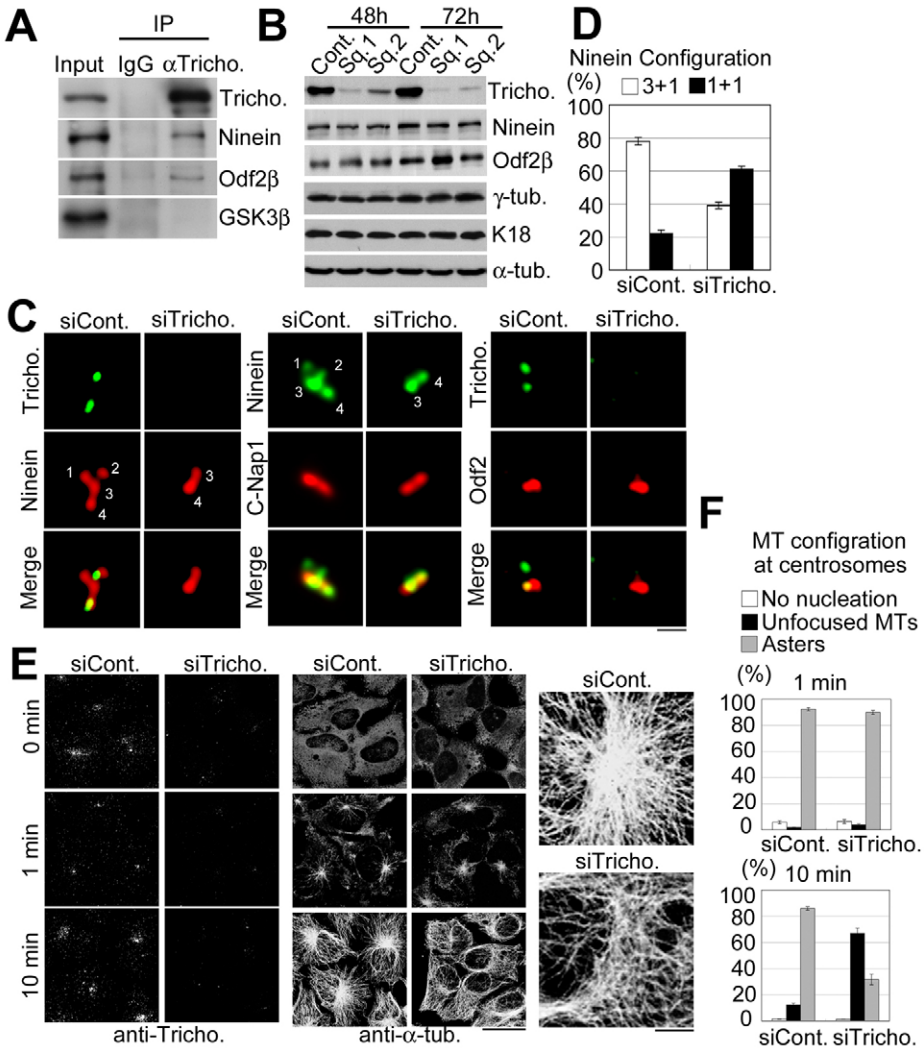

Fig. 3. Trichoplein controls ninein recruitment at appendages and microtubule anchoring at the centrosome.
(**A**) Immunoprecipitation (IP) assays using rabbit anti-human trichoplein. We used the same amount of rabbit IgG as a negative control (IgG). 2.5% of cell extract was also applied in the 'Input' lane. (**B**) HeLa cells treated with control (Cont.) or trichoplein-specific siRNA (Sq.1 or Sq.2) for 48 or 72 hours were subjected to immunoblotting with the indicated antibodies. (**C**–**F**) Effects of trichoplein depletion on localization of ninein or Odf2 (C,D) or MT regrowth assays after cold depolymerization (E,F). High magnification views on right indicate MT structures around the centrosome at 10 minutes after warming (E). Scale bars: 1 μm (10 μm for magnifications in E). Quantification data of ninein configuration (D) or MT morphology from centrosomes (F) in each group of cells are also indicated. The latter (F) were classified into the following three groups: no MT nucleation (white bars), unfocused MT network (black bars), and aster formation (gray bars). We analyzed 100 (D) or 400 (F) cells. Data are mean ± s.e.m. values from three independent experiments.

Cenexin) (Soung et al., 2006; Soung et al., 2009) and ninein in vitro (supplementary material Fig. S3B). These observations together suggest that trichoplein binds ninein and Odf2, probably through direct protein–protein interaction.

We next examined the effect of trichoplein depletion by RNA interference (RNAi). The treatment with human trichoplein-specific siRNAs induced the reduction of trichoplein protein level 48 or 72 hours after transfection (Fig. 3B). Because this treatment was unlikely to affect total protein levels of other centrosomal components such as ninein or Odf2β (Fig. 3B), we analyzed the change in their localization. As shown in Fig. 3C,D, in cells transfected with control siRNA, most anti-ninein signals were observed as three spots [which probably represent two separate signals (dots number 1 and 2) of subdistal appendages and one signal (dot number 3) of the proximal end on a mother centriole] plus one spot [which probably represents one signal (dot number 4)] at the proximal end on a daughter centriole (referred to as 3+1 patterns). However, in the trichoplein knockdown (KD) cells, anti-ninein signals diminished specifically at two spots. Because the remaining dots overlapped with C-Nap-1 (Fig. 3C), a proximal marker protein (Fry et al., 1998; Mayor et al., 2000), trichoplein depletion impaired ninein localization at the subdistal appendages of a mother centriole (dots number 1 and 2) but not at proximal ends of mother and daughter centrioles (dots number 3 and 4), which resulted in 1+1 patterns. However, the localization of Odf2 was not apparently affected by the reduction of trichoplein (Fig. 3C). These results suggest that trichoplein is required for ninein recruitment to subdistal appendages of a mother centriole but not to the proximal ends of both centrioles.

This requirement of trichoplein for ninein recruitment led us to perform MT-regrowth assays after cold depolymerization (Fig. 3E,F) (Luders et al., 2006; Yan et al., 2006), because ninein is reportedly required for MT anchoring (Dammermann and Merdes, 2002; Delgehyr et al., 2005). In cells transfected with both control siRNA and trichoplein-specific siRNA, a small centrosomal MT aster was visible 1 minute after warming. After 10 minutes, control cells had assembled an extensive array of cytoplasmic MTs that were centered at the centrosome. However, trichoplein depletion impaired this MT regrowth from the centrosome, although it did not affect the formation of cytoplasmic MTs. Trichoplein knockdown (KD) cells contained a cytoplasmic MT array that was similar in MT density to controls, but differed in that it did not have a radial, centrosome-based organization. These results suggest that trichoplein is required for MT anchoring at the centrosome.

To explore more precisely the relationships among trichoplein, ninein and Odf2, we transfected cells with ninein- (Fig. 4A,B) or Odf2-specific siRNAs (Fig. 4C,D). The reduction of ninein (Fig. 4A) or Odf2 (Fig. 4C) protein induced only marginal changes in total protein levels of the other components including trichoplein. Immunocytochemical analysis also revealed that ninein depletion induced only marginal changes in the centrosomal localization of trichoplein or Odf2 (Fig. 4B). However, Odf2 depletion abolished the recruitment of trichoplein to a mother centriole, although trichoplein localization at a daughter centriole appeared normal in Odf2 KD cells (Fig. 4D). As in trichoplein KD cells (Fig. 3C,D), anti-ninein signals diminished specifically at two spots in Odf2 KD cells (1+1 patterns; Fig. 4D,E). The rescue experiments confirmed that the observed abolition of trichoplein or ninein was attributed directly to specific depletion of trichoplein (Fig. 4F,G) or Odf2 (Fig. 4H-J), respectively. These observations suggest that Odf2 is required not only for the recruitment of trichoplein to a mother centriole, but also for ninein localization at subdistal appendages. Because the depletion of ninein or Odf2 (Fig. 4K-M) induced phenomena that were similar to those of trichoplein (Fig. 3E,F) in MT regrowth assays, we considered that Odf2, trichoplein and ninein cooperatively regulated MT anchoring at a mother centriole.

In the present study, we found that trichoplein, which was originally identified as a keratin IF scaffold protein (Nishizawa et al., 2005), is a component of centrioles at the subdistal to medial zone in proliferating cells. Ishikawa and co-workers (Ishikawa et al., 2005) reported that deletion of the Odf2 locus disrupted mother centriole appendages and eliminated two appendage-specific ninein dots, a phenomenon similar to that observed here in the case of RNAi-mediated Odf2 depletion (Fig. 4D). The present study thus indicates the way in which Odf2 controls ninein localization specifically at the subdistal appendages. Odf2 controls trichoplein localization specifically at a mother centriole (Fig. 4D) and then trichoplein recruits ninein specifically to subdistal appendages (Fig. 3C). Together with ninein (Mogensen et al., 2000; Delgehyr et al., 2005; Yan et al., 2006), trichoplein and Odf2 are indispensable to MT-anchoring activity at the centrosome (Fig. 3E,F and Fig. 4K-M). Because ninein depletion did not apparently affect the localization of two proteins (Fig. 4B), trichoplein and Odf2 might well regulate MT anchoring through the recruitment of ninein specifically to appendages. This notion is consistent with previous reports that ninein localizes to appendages and then makes a preferred docking site for MT attachment at the centrosome (Mogensen et al., 2000; Dammermann and Merdes, 2002; Ou et al., 2002; Delgehyr et al., 2005; Yan et al., 2006).

Odf2 is only required for trichoplein recruitment to the mother centriole: trichoplein localization to the presumptive daughter centriole appears normal when Odf2 is depleted (Fig. 4D). In addition, Odf2 (Fig. 4D) and trichoplein (Fig. 3C) are only indispensable for the localization of appendage-associated ninein. So, the interaction among these proteins might occur only around appendages (the subdistal end of a mother centriole) and thus be required for MT anchoring.

Since it binds Odf2 or ninein in a two-hybrid or purified protein system (supplementary material Fig. S3), trichoplein might directly engage Odf2 and appendage-associated ninein in vivo. However, this model appears to conflict with immunocytochemical observations that trichoplein does not completely overlap with Odf2 or ninein in a mother centriole (Fig. 2B). There are four possibilities to explain this: (1) the complex between trichoplein and Odf2 or ninein forms (probably in the cytoplasm) only before recruiting these proteins to a mother centriole; after the recruitment, these molecules are separated and then localized to distinct compartments; (2) other protein(s) might mediate the complex formation between trichoplein and Odf2 or ninein; (3) only a minor population of trichoplein directly binds Odf2 or ninein at a mother centriole, which is functionally more than enough; (4) trichoplein acts as a template for formation of the subdistal appendage. Regardless of these ideas, trichoplein works as a key mediator between Odf2 and appendage-associated ninein.

Odf2β and ninein reportedly regulate different cellular events (Ishikawa et al., 2005; Soung et al., 2006; Lechler and Fuchs, 2007; Moss et al., 2007; Soung et al., 2009). Odf2β depletion reduced the cell population at G1–S phase and elevated the population at S or G2–M phase (Soung et al., 2006). Because trichoplein depletion showed a similar FACS profile in HeLa cells (supplementary material Fig. S4), normal cell cycle progression

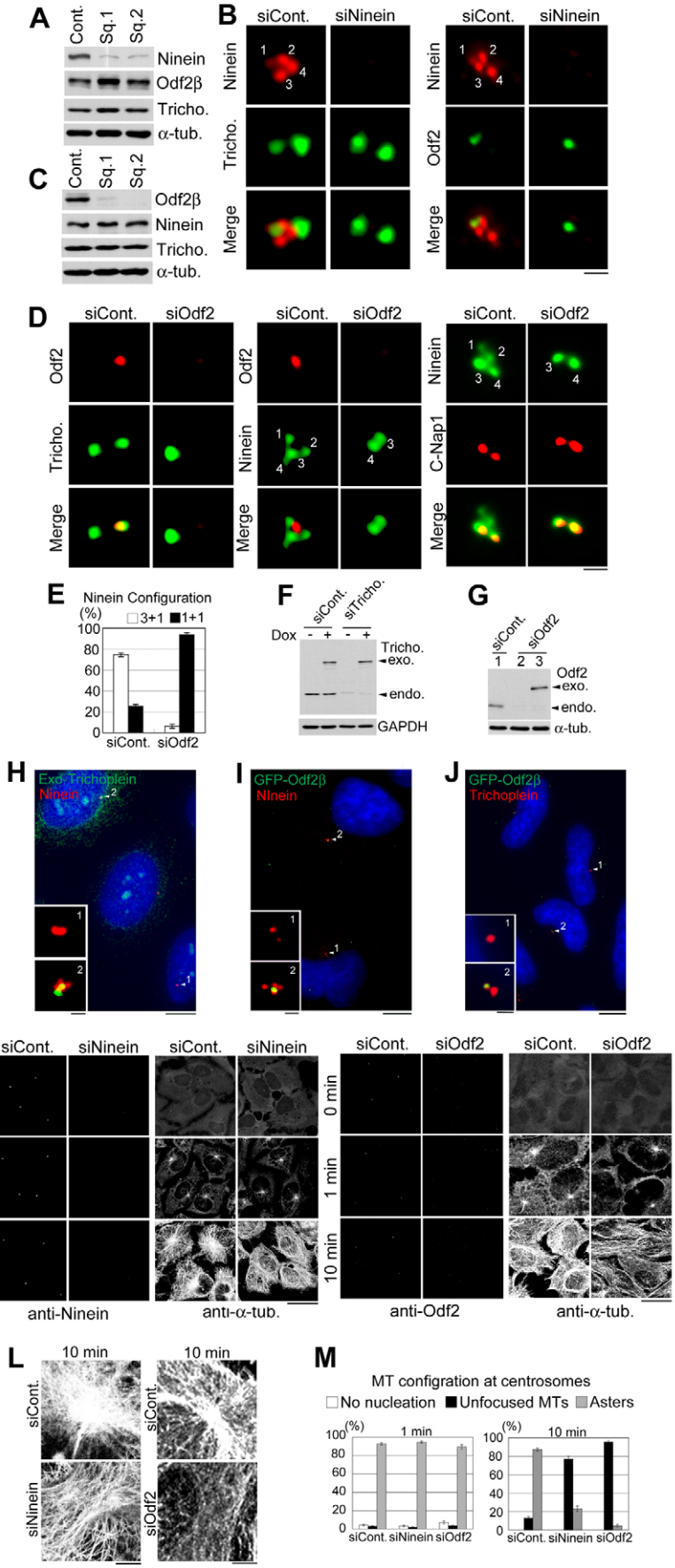

Fig. 4. Odf2 control recruitment of trichoplein and ninein at the distal end of a mother centriole. (**A**–**E**) Effects of depletion of ninein or Odf2 on other components. HeLa cells were treated with siRNAs specific to ninein (A,B) or Odf2 (C–E) for 96 hours. Then, cells were subjected to immunoblotting (A,C) or immunofluorescence (B,D) with the indicated antibodies. Scale bars: 1 μm. Quantification data of ninein configuration in each group of cells is indicated in E. (**F**,**H**) Rescue experiments of trichoplein siRNA in HeLa cells where MBP-trichoplein–FLAG is expressed in a tetracycline/doxycycline-dependent manner (Tet-ON HeLa cells). Cells were transfected with a negative control siRNA (siCont.) or trichoplein Sq.2 siRNA (targeting the 3′ UTR; siTricho.). Four hours after transfection, we removed the transfection medium and added a new growing medium with (+) or without (–; F) 100 ng/ml doxycycline. 48 hours after transfection, cells were subjected to immunoblotting with anti-trichoplein (to detect both endogenous and exogenous trichoplein) or anti-GAPDH (F) or immunofluorescence with anti-MBP (to detect only exogenous MBP-trichoplein–FLAG) and anti-ninein (H). (**G**,**I**) Rescue experiments using human-specific Odf2 siRNA2 and mouse GFP–Odf2β transfection. We transfected HeLa cells with the mixture of control (siCont.) or Odf2-specific (siOdf2) siRNA, pEGFP vector carrying mock (lanes 1, 2) or Odf2β (lane 3 in G), and Lipofectamine™ 2000 reagent. 48 hours after transfection, cells were subjected to immunoblotting with anti-Odf2 (to detect both endogenous and exogenous Odf2) or anti-α-tubulin (G) or immunofluorescence with anti-GFP (to detect only exogenous GFP–Odf2β) and anti-ninein (I) or anti-trichoplein (J). Scale bars: 1 μm (insets), 10 μm (H-J). (**K**–**M**) Effects of depletion of each protein on MT regrowth assays after cold depolymerization. Experiments were performed as described in Fig. 3E,F.

might require functional interaction between trichoplein and Odf2. However, ninein depletion had little impact on the cell cycle profile (Mikule et al., 2007), and the recruitment of ninein to appendages by Odf2 was dispensable for cell cycle regulation (Soung et al., 2009). Thus, trichoplein might regulate cell cycle progression independently of appendage-associated ninein. As for cell–cell contact, trichoplein (Fig. 1B,C and supplementary material Fig. S1A,B) (Nishizawa et al., 2005) and ninein (Lechler and Fuchs, 2007) are concentrated at the desmosome, although Odf2 does not appear to move to the cell–cell contact area (supplementary material Fig. S1C). Ninein is reported to move to desmosomes via desmoplakin and regulate MT dynamics during epidermal differentiation (Lechler and Fuchs, 2007). However, the Ca^{2+}-switch experiment revealed that trichoplein did not completely overlap with desmoplakin in the process of initial cell–cell contact formation: trichoplein appeared to be concentrated at the cell–cell contact area earlier than desmoplakin was (Fig. 1D). These observations overall suggest the possibility that trichoplein and ninein might have different roles in the formation of cell–cell contacts, at least before desmosome organization. Further studies to pursue the above possibilities and pinpoint the underlying mechanisms will be undertaken in future.

The present study documents the functional importance of a keratin IF scaffold protein trichoplein in MT anchoring at the centrosome and paves the way for future studies evaluating the inverse relationship between cell cycle progression and cell differentiation.

Materials and Methods

Preparation of recombinant proteins

His-tagged mouse trichoplein, MBP-human trichoplein or GST–ninein were expressed in BL21 CodonPlus® RP (Stratagene, La Jolla, CA) transformed with pET28a (Merck, Whitehouse Station, NJ) carrying mouse trichoplein, pMAL (New England Biolabs) carrying human trichoplein or pGEX (GE Healthcare, Milwaukee, WI) carrying ninein, respectively. We generated the recombinant baculovirus encoding GST–Odf2β using a combination of the GATEWAY™ vector conversion system and the Bac-to-Bac baculovirus expression system (Invitrogen). GST–Odf2β protein was expressed in the baculovirus-infected Sf9 cells. For production of an antibody against mouse trichoplein, His-tagged mouse trichoplein was purified on nickel-nitrilotriacetic acid-agarose resin (Qiagen; Valencia, CA) under 8 M urea denaturing conditions according to the manufacturer's protocol. For GST pull-down assay, each GST-fusion protein or MBP–trichoplein was purified under native condition through affinity chromatography with glutathione Sepharose™ 4B (GE Healthcare) or amylose resin (New England Biolabs) according to the manufacturer's protocol.

Antibodies

Anti-human and anti-mouse trichoplein antibodies were produced as described previously (Nishizawa et al., 2005). Antibodies from commercial sources were as follows: anti-centrin-2 (N-17), anti-GFP (B-2; Santa Cruz Biotechnology, Santa Cruz, CA); anti-pan-keratin, anti-keratin-18 (CY-90), anti-α-tubulin (B-5-1-2), anti-γ-tubulin (GTU-88) or anti-Odf2 (HPA001874; Sigma); anti-C-Nap1 (clone 42; BD Transduction Laboratories, San Diego, CA); anti-ninein (Poly6028; Biolegend, San Diego, CA); anti-desmoplakin-1 (DP-1), anti-desmoplakin-1/2 (clone DP1&2-2.15; DP1-2.17; DP1&2-2.20; Progen); anti-p38MAPK (#9212; Cell Signaling Technology); anti-MBP (ab9385; New England Biolabs); HRP-conjugated anti-GAPDH or anti-α-tubulin (ab15246; Abcam, Cambridge, UK); Anti-His (8916-1) or Anti-GFP (A. v. peptide; BD Clontech); and Anti-GFP (7.1 and 13.1; Roche, Basel, Switzerland). Western analyses were performed as described previously (Sugimoto et al., 2008).

Preparation of centrosomes

Centrosomes were isolated from KE37 and HeLa cells by discontinuous gradient ultracentrifugation according to the method of Moudjou and Bornens (Moudjou and Bornens, 1998). In brief, cells in the exponential phase of growth were treated with 1 μg/ml cytochalasin D and 0.2 μM nocodazole for 1 hour. Cells were collected by trypsinization and centrifugation and the resulting pellet was washed in TBS followed by 0.1× TBS with 8% sucrose. Cells were resuspended in 2 ml 0.1× TBS in 8% sucrose followed by addition of 8 ml lysis buffer (1 mM HEPES, pH 7.2, 0.5% NP-40, 0.5 mM $MgCl_2$, 0.1% β-mercaptoethanol, 1 μg/ml leupeptin, 1 μg/ml pepstatin, 1 μg/ml aprotinin and 1 mM PMSF). The suspension was gently shaken and passed five times through a 10 ml narrow-mouth serological pipette to lyse the cells. The lysate was spun at 2500 ***g*** for 10 minutes to remove swollen nuclei, chromatin aggregates and unlysed cells. The resulting supernatant was filtered through a nylon membrane followed by addition of HEPES buffer and DNaseI to a final concentration of 10 mM and 1 μg/ml, respectively, and incubated on ice for 30 minutes. The mixture was gently underlaid with 1 ml of 60% sucrose solution (10 mM PIPES pH 7.2, 0.1% Triton X-100 and 0.1% β-mercaptoethanol containing 60% w/w sucrose) and centrifuged at 10,000 ***g*** for 30 minutes to sediment centrosomes onto the cushion. The upper 8 ml of the supernatant was removed and the remainder, including the cushion containing the concentrated centrosomes, was gently vortexed and loaded onto a discontinuous sucrose gradient consisting of 70, 50, and 40% solutions from the bottom, respectively and centrifuged at 120,000 ***g*** for 1 hour. Fractions were collected and stored at –70°C before further analysis.

siRNA transfection

The following 21-nucleotide double-strand RNAs and negative controls (Negative Control and AllStars Neg. Control siRNA) were purchased from Qiagen: human trichoplein target sequence 1 (Sq.1), 5′-(AA)GAGCAGAGGAAACTGATTG-3′; human trichoplein Sq.2, 5′-(CA)GGGCATTGTTCCATGGTTA-3′; human trichoplein Sq.3, 5′-(CA)GTGTTTGGCCAGACATTAA-3′; human trichoplein Sq.4, 5′-(AA)GGCAGAATGGAGCTCTAAA-3′; mouse trichoplein Sq.5, 5′-(AA)GCTCTATCTCAGTATCAAA-3′; mouse trichoplein Sq.6, 5′-(CA)GGAATGCTTTATAAGTACA-3′; human ninein Sq.1, 5′-(CT)GGAAGAATATCGTGCACAA-3′; human ninein Sq.2, 5′-(AA)CGGGAACAAGAGAAGTTTA-3′. Human Odf2 siRNAs were purchased from Ambion (Austin, TX): Odf2 Sq.1, 5′-(CA)GGTCACTGTAAAATGAACC-3′ (11642); Odf2 Sq.2, 5′-(GA)GGTCAAGATGCAAAAAGGT-3′ (11735). We transfected cells with each siRNA using Lipofectamine™ RNAiMAX or Lipofectamine™ 2000 reagent, according to the manufacturer's protocol (Invitrogen). In some experiments, we repeated transfection(s) once or twice to increase the efficiency of reduction of each protein. Each set of experiments was performed under the same conditions including the siRNA concentration, frequency or interval of transfection and transfection reagent used. We obtained at least similar results using two target sequences of each protein (data not shown).

Plasmid transfection

We transfected cells with each set of vector(s) using Lipofectamine™ with Plus regent and Lipofectamine™ 2000 (Invitrogen) according to the manufacturer's instructions. We used pEGFP (BD Clontech) or pcDNA3 (Promega, Madison, WI) vector for the expression of EGFP-tagged or His-tagged protein, respectively.

Immunofluorescence microscopy and signal quantification

Cultured cells were grown on a coverslip coated with or without type 1 collagen (IWAKI Glass, Tokyo, Japan). KE37 suspension cells were attached on slide glasses (FRONTIER; Matsunami Glass, Osaka, Japan) before fixation. The fixation and immunostaining were performed as described previously (Sugimoto et al., 2008). Fluorescence image stacks (Fig. 3C, Fig. 4B,D and H–J) were obtained at 0.1–0.2 μm intervals in *Z*-section with an Olympus IX71 microscope equipped with a cooled charge-coupled device camera (CoolSNAP HQ; Roper Scientific, Princeton, NJ) and an UPlan SApo 100×/1.4 NA oil-immersion lens (Olympus, Tokyo, Japan) under the control of Metamorph software (Molecular Devices, Downingtown, PA). Then, the stacks were deconvolved and integrated with AutoDeblur and AutoVisualize × ver.1.4.1 (Molecular Devices). Confocal images (Fig. 1, Fig. 3E, Fig. 4K,L and supplementary material Fig. S1) were obtained as previously described (Sugimoto et al., 2008). The fluorescence intensity was determined after subtraction of the background using Zeiss AIM confocal software (Carl Zeiss, Thornwood, NY). Fig. 2B images were obtained by Delta Vision as described (Ishikawa et al., 2005). Immunohistochemistry was performed as described previously (Nishizawa et al., 2005).

Immunoprecipitation

HeLa cells (~3 ×10^6 cells) were lysed in 1 ml of lysis buffer [25 mM Tris-HCl, pH 7.5, 100 mM NaCl, 1 mM EDTA, 1 mM EGTA, 2.5 mM sodium pyrophosphate, 1 mM β-glycerophosphate, 1 mM sodium vanadate, 0.5% NP-40, 0.5% Empigen BB and protease inhibitor cocktail (Nacalai Tasque, Kyoto, Japan)] at 4°C for 10 minutes. After centrifugation (17,000 ***g***) for 20 minutes, the supernatant was incubated with rabbit polyclonal anti-human trichoplein or rabbit IgG (each 2 μg) at 4°C for 3 hours. After centrifugation (17,000 ***g***) for 20 minutes, the supernatant was rotated with 5 μl Protein-G–Sepharose™ (GE Healthcare) at 4°C for 20 minutes. After washing with lysis buffer three times, each immunoprecipitate was subjected to immunoblotting. For the detection of trichoplein, we used horseradish-peroxidase-conjugated anti-rabbit IgG (light chain-specific; Jackson ImmunoResearch Laboratories, West Grove, PA) as a secondary antibody.

GST pull-down assay

GST, GST–ninein, or GST–Odf2β (10 μg) was pre-incubated with 10 μl glutathione–Sepharose™ 4B (GE Healthcare) in binding buffer [50 mM Tris-HCl, pH 7.5, 150 mM NaCl, 1% Triton X-100, 1 mM EDTA and protease inhibitor cocktail (Nacalai Tasque)] for 1 hour at 4°C. After washing with binding buffer three times, the beads

were incubated with 10 μg MBP or MBP-trichoplein in 200 μl of the binding buffer for 1 hour at 4°C. After washing with the binding buffer three times, the beads were subjected to the immunoblotting with anti-MBP.

Establishment of Tet-ON HeLa cells

The rtTA-advanced segment and the tTS transcriptional silencer segment from pTet-On Advanced and pQC-tTS-IN (BD Clontech, Palo Alto, CA) were recombined into the retroviral vector pDEST-PQCXIP and pDEST-PQCXIN (Miyoshi et al., 1998), respectively, by the LR reaction (Invitrogen) to generate PQCXIN-Tet-On ADV and PQCXIP-tTS. The Elongation factor 1 alpha promoter (EF) in CSII-EF-MCS (a gift from Hiroyuki Miyoshi, RIKEN BioResource Center, Tsukuba, Japan) was replaced with a Tet-responsive promoter (TRE-Tight) from pTRE-Tight (BD Clontech) followed by a modified RfA fragment (Invitrogen) to make a Tet-responsive lentivirus vector, CSII-TRE-Tight-RfA. Fusion cDNAs with siRNA-resistant trichoplein were recombined into the lentiviral vector by the LR reaction (Invitrogen) to generate CSII-TRE-Tight-MBP-trichoplein-3xFLAG. Production and infection of recombinant retroviruses and lentiviruses were described as previously (Miyoshi et al., 1998; Sasaki et al., 2009).

We are grateful to Shoichiro Tsukita for providing EpH4 cells, Masatoshi Takeichi for MTD1A cells, Phillip James for pGBD-C1 and pGAD-C1 yeast two-hybrid vectors, Akira Kikuchi for providing mouse ninein cDNA and antibodies, Hiroyuki Miyoshi for CSII-EF-MCS and the related constructs, K. Kasahara for performing the immunoprecipitation in Fig. 3A, S. Yonemura and K. Kunimoto for helpful discussion, C. Yuhara and K. Kobori for technical assistance, Y. Takada for secretarial expertise, and M. Moore and J. Shields for critical comments on the manuscript. This work was supported in part by Grants-in-Aid for Scientific Research from the Japan Society for the Promotion of Science and from the Ministry of Education, Science, Technology, Sports and Culture of Japan; by a Grant-in-Aid for the Third Term Comprehensive 10-Year Strategy for Cancer Control from the Ministry of Health and Welfare, Japan; by the Uehara Memorial Foundation; by the Naito Foundation; by the Takeda Science Foundation; by a Research Grant from the Princess Takamatsu Cancer Research Fund; and by Astellas Foundation for Research on Metabolic Disorders.

Supplementary material available online at
http://jcs.biologists.org/cgi/content/full/124/6/857/DC1

References

Bettencourt-Dias, M. and Glover, D. M. (2007). Centrosome biogenesis and function: centrosomics brings new understanding. *Nat. Rev. Mol. Cell Biol.* **8**, 451-463.
Bornens, M. (2002). Centrosome composition and microtubule anchoring mechanisms. *Curr. Opin. Cell Biol.* **14**, 25-34.
Bornens, M. (2008). Organelle positioning and cell polarity. *Nat. Rev. Mol. Cell Biol.* **9**, 874-886.
Dammermann, A. and Merdes, A. (2002). Assembly of centrosomal proteins and microtubule organization depends on PCM-1. *J. Cell Biol.* **159**, 255-266.
Delgehyr, N., Sillibourne, J. and Bornens, M. (2005). Microtubule nucleation and anchoring at the centrosome are independent processes linked by ninein function. *J. Cell Sci.* **118**, 1565-1575.
Eriksson, J. E., Opal, P. and Goldman, R. D. (1992). Intermediate filament dynamics. *Curr. Opin. Cell Biol.* **4**, 99-104.
Eriksson, J. E., Dechat, T., Grin, B., Helfand, B., Mendez, M., Pallari, H. M. and Goldman, R. D. (2009). Introducing intermediate filaments: from discovery to disease. *J. Clin. Invest.* **119**, 1763-1771.
Fry, A. M., Mayor, T., Meraldi, P., Stierhof, Y. D., Tanaka, K. and Nigg, E. A. (1998). C-Nap1, a novel centrosomal coiled-coil protein and candidate substrate of the cell cycle-regulated protein kinase Nek2. *J. Cell Biol.* **141**, 1563-1574.
Fuchs, E. and Cleveland, D. W. (1998). A structural scaffolding of intermediate filaments in health and disease. *Science* **279**, 514-519.
Fuchs, E. and Weber, K. (1994). Intermediate filaments: structure, dynamics, function, and disease. *Annu. Rev. Biochem.* **63**, 345-382.
Godsel, L. M., Hobbs, R. P. and Green, K. J. (2008). Intermediate filament assembly: dynamics to disease. *Trends Cell Biol.* **18**, 28-37.
Houseweart, M. K. and Cleveland, D. W. (1998). Intermediate filaments and their associated proteins: multiple dynamic personalities. *Curr. Opin. Cell Biol.* **10**, 93-101.
Ishikawa, H., Kubo, A. and Tsukita, S. (2005). Odf2-deficient mother centrioles lack distal/subdistal appendages and the ability to generate primary cilia. *Nat. Cell Biol.* **7**, 517-524.
Izawa, I. and Inagaki, M. (2006). Regulatory mechanisms and functions of intermediate filaments: a study using site- and phosphorylation state-specific antibodies. *Cancer Sci.* **97**, 167-174.
Lange, B. M. and Gull, K. (1995). A molecular marker for centriole maturation in the mammalian cell cycle. *J. Cell Biol.* **130**, 919-927.
Laoukili, J., Perret, E., Middendorp, S., Houcine, O., Guennou, C., Marano, F., Bornens, M. and Tournier, F. (2000). Differential expression and cellular distribution of centrin isoforms during human ciliated cell differentiation in vitro. *J. Cell Sci.* **113**, 1355-1364.
Lechler, T. and Fuchs, E. (2007). Desmoplakin: an unexpected regulator of microtubule organization in the epidermis. *J. Cell Biol.* **176**, 147-154.
Luders, J., Patel, U. K. and Stearns, T. (2006). GCP-WD is a gamma-tubulin targeting factor required for centrosomal and chromatin-mediated microtubule nucleation. *Nat. Cell Biol.* **8**, 137-147.
Magin, T. M., Vijayaraj, P. and Leube, R. E. (2007). Structural and regulatory functions of keratins. *Exp. Cell Res.* **313**, 2021-2032.
Mayor, T., Stierhof, Y. D., Tanaka, K., Fry, A. M. and Nigg, E. A. (2000). The centrosomal protein C-Nap1 is required for cell cycle-regulated centrosome cohesion. *J. Cell Biol.* **151**, 837-846.
Mikule, K., Delaval, B., Kaldis, P., Jurcyzk, A., Hergert, P. and Doxsey, S. (2007). Loss of centrosome integrity induces p38-p53-p21-dependent G1-S arrest. *Nat. Cell Biol.* **9**, 160-170.
Miyoshi, H., Blomer, U., Takahashi, M., Gage, F. H. and Verma, I. M. (1998). Development of a self-inactivating lentivirus vector. *J. Virol.* **72**, 8150-8157.
Mogensen, M. M., Malik, A., Piel, M., Bouckson-Castaing, V. and Bornens, M. (2000). Microtubule minus-end anchorage at centrosomal and non-centrosomal sites: the role of ninein. *J. Cell Sci.* **113**, 3013-3023.
Moss, D. K., Bellett, G., Carter, J. M., Liovic, M., Keynton, J., Prescott, A. R., Lane, E. B. and Mogensen, M. M. (2007). Ninein is released from the centrosome and moves bi-directionally along microtubules. *J. Cell Sci.* **120**, 3064-3074.
Moudjou, M. and Bornens, M. (1998). Method of centrosome isolation from cultured animal cells. In *Cell Biology: A Laboratory Handbook* (ed. J. E. Celis), 111 pp. Orlando, FL: Academic Press Inc.
Nakagawa, Y., Yamane, Y., Okanoue, T. and Tsukita, S. (2001). Outer dense fiber 2 is a widespread centrosome scaffold component preferentially associated with mother centrioles: its identification from isolated centrosomes. *Mol. Biol. Cell* **12**, 1687-1697.
Nigg, E. A. and Raff, J. W. (2009). Centrioles, centrosomes, and cilia in health and disease. *Cell* **139**, 663-678.
Nishizawa, M., Izawa, I., Inoko, A., Hayashi, Y., Nagata, K., Yokoyama, T., Usukura, J. and Inagaki, M. (2005). Identification of trichoplein, a novel keratin filament-binding protein. *J. Cell Sci.* **118**, 1081-1090.
Ou, Y. Y., Mack, G. J., Zhang, M. and Rattner, J. B. (2002). CEP110 and ninein are located in a specific domain of the centrosome associated with centrosome maturation. *J. Cell Sci.* **115**, 1825-1835.
Paoletti, A., Moudjou, M., Paintrand, M., Salisbury, J. L. and Bornens, M. (1996). Most of centrin in animal cells is not centrosome-associated and centrosomal centrin is confined to the distal lumen of centrioles. *J. Cell Sci.* **109**, 3089-3102.
Pekny, M. and Lane, E. B. (2007). Intermediate filaments and stress. *Exp. Cell Res.* **313**, 2244-2254.
Sasaki, R., Narisawa-Saito, M., Yugawa, T., Fujita, M., Tashiro, H., Katabuchi, H. and Kiyono, T. (2009). Oncogenic transformation of human ovarian surface epithelial cells with defined cellular oncogenes. *Carcinogenesis* **30**, 423-431.
Soung, N. K., Kang, Y. H., Kim, K., Kamijo, K., Yoon, H., Seong, Y. S., Kuo, Y. L., Miki, T., Kim, S. R., Kuriyama, R. et al. (2006). Requirement of hCenexin for proper mitotic functions of polo-like kinase 1 at the centrosomes. *Mol. Cell. Biol.* **26**, 8316-8335.
Soung, N. K., Park, J. E., Yu, L. R., Lee, K. H., Lee, J. M., Bang, J. K., Veenstra, T. D., Rhee, K. and Lee, K. S. (2009). Plk1-dependent and -independent roles of an ODF2 splice variant, hCenexin1, at the centrosome of somatic cells. *Dev. Cell* **16**, 539-550.
Steinert, P. M. (1993). Structure, function, and dynamics of keratin intermediate filaments. *J. Invest. Dermatol.* **100**, 729-734.
Sugimoto, M., Inoko, A., Shiromizu, T., Nakayama, M., Zou, P., Yonemura, S., Hayashi, Y., Izawa, I., Sasoh, M., Uji, Y. et al. (2008). The keratin-binding protein Albatross regulates polarization of epithelial cells. *J. Cell Biol.* **183**, 19-28.
Yan, X., Habedanck, R. and Nigg, E. A. (2006). A complex of two centrosomal proteins, CAP350 and FOP, cooperates with EB1 in microtubule anchoring. *Mol. Biol. Cell* **17**, 634-644.